An Analysis of the Effect of Fault Location on the Transient Stability of a PV-Integrated IEEE 30 Bus System with FACTS Devices

Mohammed Soufiane Chekembou
Department of Electrical Engineering, LACoSERE Laboratory, Amar Telidji University of Laghouat, Algeria
m.chekembou@lagh-univ.dz (corresponding author)

Mohammed Omrane
Department of Electrical Engineering, LACoSERE Laboratory, Amar Telidji University of Laghouat, Algeria
m.omrane@lagh-univ.dz

Lakhdar Mokrani
Department of Electrical Engineering, LACoSERE Laboratory, Amar Telidji University of Laghouat, Algeria
l.mokrani@lagh-univ.dz

Ali Medjghou
Department of Electronics, Faculty of Science, University of Tipaza, Algeria | Department of Electronics, LAAAS Laboratory, University of Batna 2, Algeria
medjghou.ali@gmail.com

Djemai Naimi
Department of Electrical Engineering, LGEB Laboratory, University of Biskra, Algeria
d.naimi@univ-biskra.dz

Khaled Miloudi
Department of Mechanical Engineering, Faculty of Technology, University of El Oued, Algeria
miloudi-khaled@univ-eloued.dz

Received: 21 December 2025 | Revised: 11 January 2026 and 19 January 2026 | Accepted: 23 January 2026

 DOI: https://doi.org/10.48084/etasr.17081

ABSTRACT

The increasing penetration of PhotoVoltaic (PV) generation in power systems has become a serious concern regarding transient stability under severe fault conditions. In this study, the effect of fault location on the transient stability of a PV-integrated IEEE 30-bus system was analyzed using the Critical Clearing Time (CCT) as a stability index. A 50 MW PV unit was connected to the selected bus, and several three-phase fault scenarios were simulated using MATLAB/Power System Analysis Toolbox (PSAT). To improve system stability, three Flexible AC Transmission System (FACTS) devices, namely, Static Var Compensator (SVC), Static Synchronous Compensator (STATCOM), and Unified Power Flow Controller (UPFC), were implemented and compared. The obtained results show that transient stability is highly sensitive to fault location, even in the absence of PV integration. The presence of PV generation decreases the CCT and incurs high sensitivity to fault clearing time, especially at a weak bus. The application of FACTS devices enhanced the transient stability and increased the CCT for all considered cases. UPFC is the most effective and reliable device for enhancing system stability, followed by STATCOM, whereas SVC has a limited effect, depending on the fault location.

Keywords-transient stability; fault location; critical clearing time; photovoltaic integration; FACTS devices; IEEE 30-bus system

I. INTRODUCTION

The integration of PV systems into power grids, driven by advancements in control and power electronics, introduces challenges to transient stability due to reduced system inertia and altered damping characteristics [1, 2]. This affects the CCT, with weaker grids experiencing more significant reductions in stability margins [3-6]. High PV penetration leads to lower CCT, influenced by PV integration location and grid strength [7, 8]. To reduce the adverse effects of PV integration on transient stability, various FACTS devices, like SVC, STATCOM, and UPFC have been widely studied. These devices provide fast reactive power support and dynamic voltage control, improving stability during faults [9, 10]. Among them, UPFC has shown superior performance due to its series–shunt control capability [11]. However, the combined effect of fault location, PV placement, and FACTS performance on transient stability remains insufficiently explored, especially the sensitivity of CCT to fault location in PV-integrated systems with FACTS devices. While fault location impacts on CCT are well established in conventional systems [12] and increasingly relevant in inverter-based grids [6], FACTS devices, such as STATCOM and UPFC, have mainly been studied independently for stability enhancement in renewable-integrated power systems [9, 13, 14]. The critical role of FACTS controllers in modern power system stability has been further highlighted [15].

Despite these advancements, a distinct research gap persists. Studies focusing on fault location sensitivity, such as [16], often analyze conventional generation systems without significant PV integration. However, research evaluating FACTS devices for renewable energy integration [13, 14] frequently considers a limited set of fault contingencies or a single type of renewable source. Consequently, a systematic investigation that explicitly evaluates CCT sensitivity across multiple fault locations, under varying PV integration scenarios, while conducting a direct performance comparison of multiple FACTS devices (SVC, STATCOM, and UPFC) has not been thoroughly conducted.

The main contribution of the current study resides in the proposed integrated sensitivity analysis framework. This study methodically investigates the impact of six different fault locations on the transient stability (quantified by CCT) of the IEEE 30-bus test system, while considering two distinct PV integration points that represent different electrical strengths within the network. Moreover, it provides a direct comparative assessment of the efficacy of three different FACTS devices (SVC, STATCOM, and UPFC) in mitigating stability degradation under these combined conditions. The outcomes of this work are intended to provide more definitive guidelines for the coordinated planning of PV systems and FACTS devices to bolster power grid resilience. Specifically, this study contributes by (i) revealing the strong nonlinear sensitivity of CCT to fault location in inverter-dominated networks, (ii) demonstrating that the PV penetration level alone is insufficient to characterize transient stability, and (iii) providing a direct and quantitative comparison of SVC, STATCOM, and UPFC under identical operating conditions. These contributions extend existing literature by offering new insights into the coordinated planning of renewable integration and dynamic compensation for enhanced system resilience.

II. METHODOLOGY

The proposed methodology is based on time-domain transient stability simulations performed on the IEEE 30-bus test system using MATLAB/PSAT [17]. The IEEE 30-bus system consists of 30 buses, 6 synchronous generators located at buses 1, 2, 5, 8, 11, and 13, 41 transmission lines, and 4 on-load tap-changing transformers, with a system base power of 100 MVA and nominal voltage levels up to 132 kV. Owing to its moderate size and popular application in stability studies, the benchmark system can demonstrate the dynamic performance under severe disturbance with acceptable numerical burden.

A. PV System Modeling

In order to assess the impact of renewable energy integration, a 50 MW PV unit was connected to the system at two different bus locations (Bus 12 and Bus 18). The buses were selected to represent different electrical strength and sensitivity of the network. PV generator can be modeled by the following single-diode equivalent model, which represents the electrical behavior of a PV cell under various operating conditions [18]. The output current–voltage relationship is expressed by:

$$I_{out} = I_{ph} - I_D - I_{sh} \quad (1)$$

$$I_{out} = I_{ph} - I_0\left[e^{\frac{q(V_{out}+I_{out}R_{se})}{\eta kT}} - 1\right] - \frac{(V_{out}+I_{out}R_{se})}{R_{sh}} \quad (2)$$

where I_{ph} is the photocurrent produced by the solar cell, I_0 is the reverse saturation current, R_{se} and R_{sh} are the series and shunt resistances, respectively. V_{out}, q, η, T, and k indicate the output voltage, electron charge, ideality factor, operational temperature, and Boltzmann constant, respectively. D is the cell photocurrent, and I_{sh} is the current through the shunt resistor. I_D denotes the current flowing through the diode.

The PV system inverter interface is modeled as a Voltage Source Converter (VSC) with a Phase-Locked Loop (PLL) and inner current control loops to regulate active and reactive power exchange with the grid [19]. This modeling approach is widely adopted for the transient stability studies of grid-connected PV systems and provides a realistic representation of inverter-based generation dynamics.

B. Transient Stability Assessment

Transient stability is assessed by imposing severe three-phase symmetrical faults at selected critical bus locations, namely, Bus 2, Bus 4, Bus 5, Bus 8, Bus 12, and Bus 18. Bus 2 is included as a critical generator bus in the base system to assess the impact of faults near traditional generation. For each fault case, the fault was gradually imposed for a longer

duration until the system experienced a loss of synchronism, and the corresponding fault clearing time was obtained as the CCT, which is the main stability performance index of this study. The CCT is related to the critical clearing angle which can be estimated using the Equal Area Criterion (EAC). Although the EAC is strictly applicable to Single-Machine Infinite Bus (SMIB) systems, it provides physical insights to the multi-machine system when some simplifying assumptions are made. The EAC is described by the energy-based formulation shown in [20]:

$$\int_{\delta_0}^{\delta_{cr}}(P_m - P_e)\,\mathrm{d}\delta = \int_{\delta_{cr}}^{\delta_{max}}(P_e - P_m)\,d\delta \quad (3)$$

where P_m is the mechanical power input, P_e is the electrical power output, δ_0 is the initial rotor angle, δ_{cr} is the critical rotor angle, and δ_{max} is the maximum rotor swing angle. The approximate expression for CCT is given by:

$$CCT = \sqrt{\frac{2H}{\omega_s(P_{acc})}}(\delta_{cr} - \delta_0) \quad (4)$$

where H is the generator inertia constant, ω_s is the synchronous speed, and $P_{acc} = P_m - P_e$ is the accelerating power.

C. FACTS Devices Modeling

To improve transient stability, three FACTS devices (SVC, STATCOM, and UPFC) were implemented and evaluated within the PSAT environment, utilizing its standard dynamic model library. Their core operational principles are mathematically summarized below.

1) SVC

The SVC is modeled as a shunt-connected, thyristor-controlled variable susceptance, B_{svc} . It provides voltage support by dynamically adjusting its reactive power injection/absorption according to:

$$Q_{svc} = -V_k^2 \times B_{svc} \quad (5)$$

where V_k is the voltage at the connected bus k. This SVC representation follows the standard dynamic model implemented in the PSAT library and is widely adopted in transient stability studies [21].

2) STATCOM

The STATCOM is modeled as a VSC connected in shunt. Its primary function is to regulate the bus voltage by injecting or absorbing reactive current. The fundamental steady-state relationship for the reactive power exchange of an ideal STATCOM can be expressed as [3, 13]:

$$Q_{statcom} = (V_k \times V_{vsc}/X) \times sin(\delta_{vsc} - \theta_k) \quad (6)$$

where $V_{vsc}\angle\delta_{vsc}$ is the controllable output voltage of the VSC, $V_k\angle\theta_k$ is the bus voltage, and X is the coupling transformer reactance. In this study's simulations, a standard PSAT VSC model with an inner current control loop and an outer voltage/reactive power control loop was employed.

3) UPFC

The UPFC is the most versatile device, combining a shunt-connected STATCOM and a series-connected static synchronous series compensator via a common DC link [5, 14]. This configuration allows for simultaneous and independent control of the voltage magnitude (via the shunt converter) and active/reactive power flow (via the series converter). The PSAT model implements this dual VSC structure, enabling coordinated control of the bus voltage and line impedance/power flow.

D. FACTS Device Implementation Assumptions

To enable a consistent and fair comparative analysis, the following assumptions were made for the implementation of the SVC, STATCOM, and UPFC:

- Number and placement: A single device of each type was evaluated independently. All devices were connected to Bus 12, which is the point of common coupling for the PV system in the primary study cases. This location was chosen as a critical node requiring voltage support and reactive power management following PV integration, allowing for a direct comparison of device efficacy under identical network conditions.
- Rated capacity and control parameters: The shunt devices (SVC, STATCOM shunt converter) were assigned a nominal dynamic range of ±50 MVar, aligning with the scale of the integrated 50 MW PV plant. The UPFC's series and shunt converters were sized with similar MVA ratings. The control parameters (e.g., proportional and integral gains, time constants) were set to standard values proposed in the PSAT documentation and aligned with those used in comparable stability studies [14] to ensure stable and well-damped dynamic performance.
- Impact on steady-state power flow: The incorporation of each FACTS device modifies the network's admittance matrix and/or bus voltage setpoints. Consequently, a fresh AC power flow calculation was performed for each system configuration (e.g., base case, PV integrated, PV integrated with STATCOM) prior to transient stability simulation. This step ensures that the pre-fault initial conditions accurately reflect the altered power flows, voltage profiles, and generator outputs resulting from the steady-state operation of the FACTS device.

Using the proposed methodology, this work systematically analyzed how transient stability is affected by fault location, PV integration, and FACTS devices. Figure 1 illustrates the IEEE 30-bus test system used in this study. The results are presented and discussed in the following sequence: first, the base case power flow (Table I), second, the sensitivity of the CCT, third, the impact of PV integration, and finally, the performance enhancement provided by different FACTS devices.

Table I presents the voltage magnitude and angle phase, the active and reactive power generated, and the active demand for each bus. These results represent the steady-state operating point of the power system without disturbances or PV integration. They provide reference values to evaluate the dynamic response of the system and to study its stability with the impact of PV penetration and the use of FACTS devices.

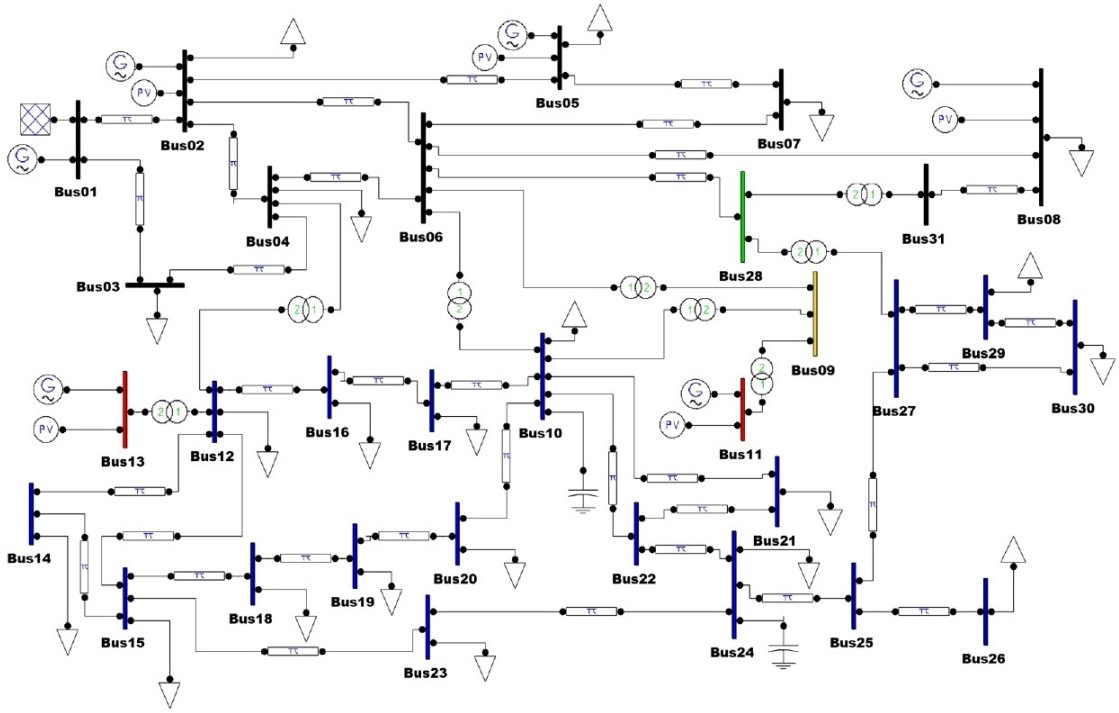

Fig. 1. IEEE 30-bus test system.

TABLE I. POWER FLOW RESULTS OF IEEE 30-BUS SYSTEM

Bus	V (p.u)	Phase (p.u)	Pgen (p.u)	Qgen (p.u)	Pload (p.u)
1	1.06	0	2.115	-0.16383	0
2	1.045	-0.07733	0.4	0.37491	0.217
3	1.0316	-0.11333	0	0	0.024
4	1.0247	-0.13638	0	0	0.076
5	1.01	-0.20995	0.1	0.27731	0.942
6	1.0182	-0.1596	0	0	0
7	1.0071	-0.18942	0	0	0.228
8	1.01	-0.16614	0.1	0.15577	0.3
9	1.051	-0.1971	0	0	0
10	1.0384	-0.22864	0	0	0.058
11	1.082	-0.18549	0.12	0.30524	0
12	1.0375	-0.21557	0	0	0.112
13	1.071	-0.20045	0.12	0.2574	0
14	1.0275	-0.23042	0	0	0.062
15	1.0282	-0.23277	0	0	0.082
16	1.0348	-0.22274	0	0	0.035
17	1.0323	-0.23057	0	0	0.09
18	1.0196	-0.24364	0	0	0.032
19	1.0176	-0.2467	0	0	0.095
20	1.022	-0.24321	0	0	0.022
21	1.0251	-0.23679	0	0	0.175
22	1.0254	-0.23664	0	0	0
23	1.0172	-0.24048	0	0	0.032
24	1.01	-0.24408	0	0	0.087
25	0.99899	-0.23984	0	0	0
26	0.98098	-0.24744	0	0	0.035
27	1.0009	-0.23263	0	0	0
28	1.0136	-0.1686	0	0	0
29	0.9806	-0.25509	0	0	0.024
30	0.96884	-0.27123	0	0	0.106

III. RESULTS AND DISCUSSION

A. Effect of Fault Location on Transient Stability (Base Case)

The simulation results in Figure 2 show that the transient stability of the IEEE 30-bus system is dependent on the fault location. The CCT varied significantly from one bus to another, indicating non-uniform strength across the network. Faults occurring near electrically weak buses or close to generator terminals result in lower CCT values, whereas faults at stronger buses exhibit higher tolerance.

In the base case without PV integration, the lowest CCT values are observed at Bus 2 (15 ms) and Bus 4 (19 ms), whereas Bus 8 (40 ms) presents the highest stability margins. Intermediate CCT values were obtained at Bus 20. These results confirm that fault location alone has a major impact on transient stability, even in conventional power systems.

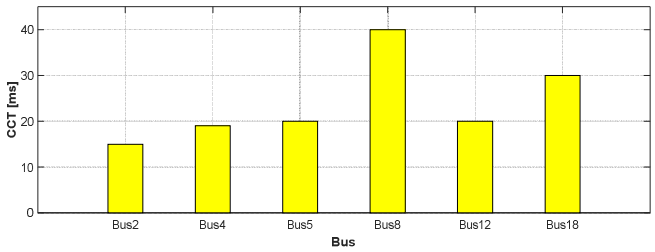

Buses	Bus2	Bus4	Bus5	Bus8	Bus12	Bus18
CCT [ms]	15	19	20	40	20	30

Fig. 2. CCT comparison without PV integration.

B. Impact of PV Integration on Transient Stability

Figure 3 shows that at t = 3 ms, the rotor speeds exhibit moderate, symmetrical variations ranging from 0.97 p.u. to 1.045 p.u., and the system clearly stabilizes after 0.65 s.

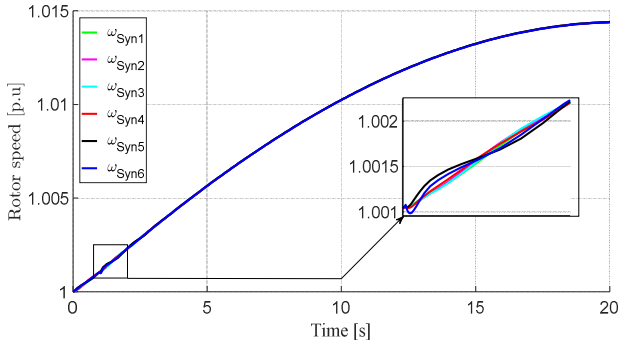

Fig. 3. Rotor speed of all generators for a three-phase fault at Bus 18, cleared at t = 3 ms (at the CCT).

It can be inferred that synchronism between the generators was maintained and that the system was within the limits of the CCT.

Figure 4 demonstrates that for t = 4 ms, the oscillations are more severe, with speeds of 1.08 and 0.92 p.u., damping is reduced, and the system almost desynchronizes two generators for about 0.8 s. Although the system does not become unstable, it operates very close to the dynamic stability limit. This shows the high sensitivity of the system to even a very small increase in the fault clearing time.

Figure 5 provides a direct visual demonstration of/depicts the CCT significance by contrasting the system voltage response at Bus 2 when the same three-phase fault is cleared at the CCT (3 ms) versus 1 ms beyond it (4 ms). When the fault is cleared precisely at the CCT (red dashed curve), the system operates at the brink of stability.

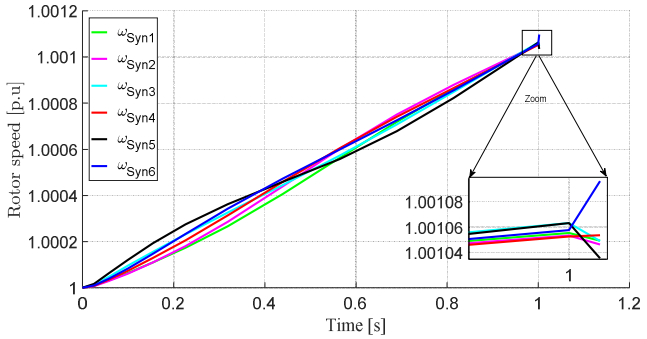

Fig. 4. Rotor speed of all generators for a three-phase fault at Bus 18, cleared at t = 4 ms (1 ms beyond the CCT).

The voltage recovers but exhibits sustained, poorly-damped oscillations, indicating a very low stability margin. The system eventually remains synchronized. Clearing the fault just 1 ms later (at t = 4 ms, blue solid curve) pushes the system into an unstable region. The voltage either fails to recover, collapsing to a new low equilibrium, or enters a growing oscillatory mode, both of which signify the loss of synchronism. This contrast between the red and blue curves visually defines the CCT's significance: an extra millisecond of fault duration can be the difference between a stable, recoverable system and a blackout. Figure 5 thus validates the proposed CCT measurement methodology and underscores the extreme sensitivity of the system, especially with PV integration to fault clearing speed, justifying the need for fast support provided by FACTS devices, as analyzed subsequently.

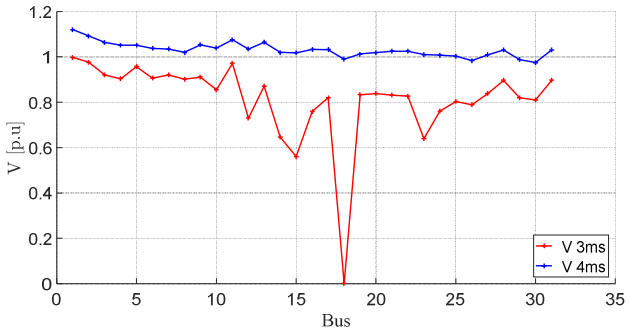

Fig. 5. Voltage profile at Bus 18 for a three-phase fault, comparing clearance at the CCT = 3 ms and 1 ms beyond it (t = 4 ms).

The CCTs obtained in this study, particularly in the range of 3-9 ms for both the base and PV-integrated cases, are notably short, primarily due to the severe fault assumption adopted in the simulations, a bolted three-phase short-circuit with zero impedance, which represents the most challenging contingency for transient stability. These values reflect the system's critical stability threshold during the initial electrical transient, before the inertial response of synchronous machines and slower control loops can provide significant damping. Such low CCTs are consistent with first-cycle stability analyses in power systems with high penetration of inverter-based resources, where the initial rate of change of frequency is extremely high [6], underscoring the need for ultra-fast protection schemes and dynamic voltage support in modern grids.

In Table II, it is demonstrated that CCT is different at six bus locations, with different levels of solar power or PV being used. This shows that using solar power does not always mean that the system will be more stable when something goes wrong. For example, Bus 2 and Bus 4 both have 23% power, but they have very low CCTs of 3 ms and 4 ms. This suggests that if something goes wrong, the system may not be able to handle it well when solar power does not work well with the rest of the network. The solar power integration at Bus 2 and Bus 4 is not properly coordinated with the network conditions, which is why reduced fault tolerance is observed at these locations, specifically at Bus 2 and Bus 4, with their respective low CCTs. In contrast, Bus 5 and Bus 8, despite having only 6% PV penetration, achieved higher CCTs of 8 ms and 9 ms, highlighting the dominant role of network strength and local system characteristics over PV penetration level alone. Similarly, Bus 12 and Bus 18, both with 7% PV penetration, show contrasting CCTs of 7 ms and 3 ms, respectively, where

the lower value at Bus 18 reflects greater sensitivity to transient disturbances, while the moderate CCT at Bus 12 suggests that appropriately located and well-integrated PV resources can positively contribute to transient stability.

TABLE II. VARIATION OF CCT ACCORDING TO PV PENETRATION

Bus	2	4	5	8	12	18
Active power (MW)	0.2	0.2	0.05	0.05	0.06	0.06
PV penetration (%)	23	23	6	6	7	7
CCT (ms)	3	4	8	9	7	3

Overall, the results indicate that the influence of solar PV on system stability exhibits nonlinear characteristics and is highly dependent on the integration point within the network. Increasing the transient stability of the system with PV integration requires not only increasing the renewable capacity, but also placing it in the right location with good grid support and inverter control to ensure a new and resilient power system under faulted conditions. The integration of a 50 MW PV unit led to a significant reduction in the CCT across most fault locations. This reduction was attributed to the inverter-based nature of PV generation and the associated decrease in effective system inertia. The system becomes highly sensitive to fault clearing time, where a small increase beyond the critical threshold may cause loss of synchronism.

Figure 6 compares the CCT at various bus positions under two cases: with and without PV integration. The results indicate that PV does not always enhance transient stability. At buses such as Bus2, Bus4, and Bus5, CCT increases, reflecting an improved system capability to withstand faults and respond dynamically. In contrast, at Bus8, CCT drops, probably because of poor grid conditions and restrictions in inverter control, whereas at Bus12 and Bus18, the rise in CCT is slight. These results indicate that the effects of PV integration are greatly influenced by location, system features, and control methods. Buses with lower electrical strength exhibit more significant effects, while those with greater strength display comparatively minor changes. Therefore, the stability benefits of PV penetration are not directly proportional to the installed capacity but are largely determined by the connection location.

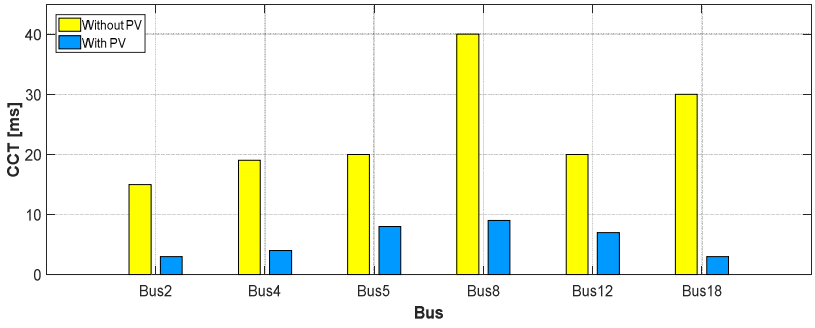

Buses	Bus2	Bus4	Bus5	Bus8	Bus12	Bus18
CCT without PV [ms]	15	19	20	40	20	30
CCT with PV [ms]	3	4	8	9	7	3

Fig. 6. CCT comparison with and without PV integration.

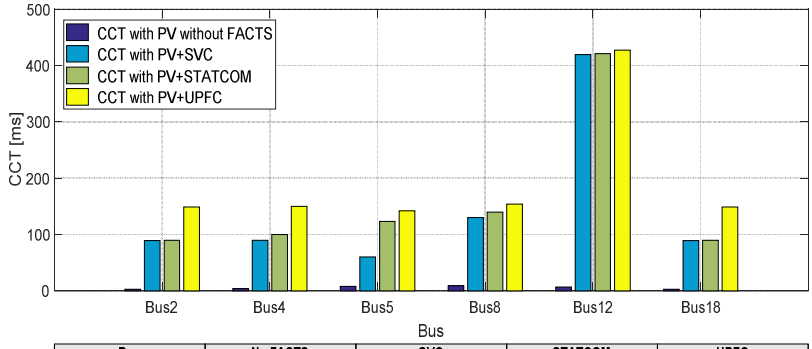

Bus	No FACTS	SVC	STATCOM	UPFC
Bus2	3	89	90	149
Bus4	4	90	100	150
Bus5	8	60	123	142
Bus8	9	130	140	154
Bus12	7	419	421	427
Bus18	3	89	90	149

Fig. 7. CCT comparison for different FACTS devices in PV-integrated system.

C. Effect of FACTS Devices on Stability Enhancement

The simulation results, as shown in Figure 7, indicate that the integration of any of the FACTS devices significantly increases the CCT value at all bus places compared to the base case (PV only). The higher CCT values (e.g., CCT values greater than 400 ms) realized in the presence of FACTS devices are due to the fast dynamic response and additional voltage support provided by VSC-based compensators [11]. Unlike the base case or PV-only case, the presence of the STATCOM and UPFC improved the post-fault voltage recovery and reduced the accelerating power during fault clearing time, which resulted in a significant increase in the CCT beyond the typical values found in uncompensated systems.

The data show that there is a significant increase in the CCT of all buses when compensating devices are added to the PV source. STATCOM significantly improves the CCT values, especially in the weakest buses, such as Bus 12 and Bus 8, (from 7 to 421, and from 9 to 140, respectively), indicating the good capability of STATCOM in voltage support and transient fault tolerance. SVC results are mixed; while for most buses it increases the CCT significantly, on Bus 5 it has poor performance, indicating a specific site issue or control problems. For most buses, UPFC improves the CCT the most compared to STATCOM and SVC, with the highest values at Bus 12 and **B**us 8 (427 and 154, respectively) indicating the highest power flow and voltage control capability of all. All CCT values above 100 ms occurred only in the FACTS device cases, whereas the base and PV-only values were in the normal millisecond range. In the weakest buses, with the least CCT for PV only (Bus 2 and Bus 18 at 3 ms), the effect of the compensators on the CCT was substantial for all compensators, but again, the UPFC provided the greatest benefit. These results indicate the important role of FACTS devices in improving the transient stability of PV-integrated power systems and the importance of selecting the right device (and location) based on the network characteristics and penetration point of the PV. The use of FACTS devices significantly enhances the transient stability of systems integrated with PV. Each device considered increased the CCT values compared to systems with only PV, demonstrating their effectiveness in counteracting the stability issues introduced by renewable integration.

Among the devices assessed, the SVC offers limited improvement, with its effectiveness varying based on where it is installed. The STATCOM provides a greater increase in CCT due to its rapid dynamic voltage support capabilities. The UPFC consistently delivers the most significant enhancement in stability margins across all fault locations, thanks to its combined control over voltage, phase angle, and power flow.

In summary, although all FACTS devices improve transient stability, the UPFC stands out for its robust and consistent performance in PV-integrated systems.

IV. CONCLUSIONS

This study presents a novel integrated sensitivity analysis of transient stability in a PhotoVoltaic (PV)-integrated IEEE 30-bus system by simultaneously considering multiple fault locations, different PV integration points, and a direct comparative assessment of three Flexible AC Transmission System (FACTS) devices. Unlike most existing studies that analyze these factors separately, the proposed framework reveals the strong nonlinear dependence of Critical Clearing Time (CCT) on both fault location and PV siting.

The results demonstrate that the PV penetration level alone is not a reliable indicator of transient stability and that fault location and network strength remain dominant factors even in inverter-dominated systems. The comparative analysis further provides new quantitative evidence on the relative effectiveness of FACTS devices, confirming the superior and more consistent performance of the Unified Power Flow Controller (UPFC), followed by the Static Synchronous Compensator (STATCOM), whereas the Static Var Compensator (SVC) exhibits a more location-dependent behavior.

These findings offer a unified and practical methodology for stability-oriented planning of renewable-rich power systems and provide engineering guidelines for the coordinated deployment of PV generation and FACTS controllers under severe fault conditions.

Future studies should examine coordinated control schemes and advanced control methods to further improve resilience during major disturbances.

REFERENCES

[1] S. Behera *et al.*, "A comprehensive study on energy management, sensitivity analysis, and inertia compliance of feed-in tariff in IEEE bus systems with grid-connected renewable energy sources," *Heliyon*, vol. 10, no. 17, Sept. 2024, Art. no. e36927, https://doi.org/10.1016/j.heliyon.2024.e36927.

[2] R. Zhu, K. Das, P. E. Sørensen, and A. D. Hansen, "A Review on Energy Management System for Grid-Connected Utility-Scale Renewable Hybrid Power Plants," *WIREs Energy and Environment*, vol. 14, no. 1, 2025, Art. no. e70004, https://doi.org/10.1002/wene.70004.

[3] Q.-H. Wu, Y. Lin, C. Hong, Y. Su, T. Wen, and Y. Liu, "Transient Stability Analysis of Large-scale Power Systems: A Survey," *CSEE Journal of Power and Energy Systems*, vol. 9, no. 4, pp. 1284–1300, Dec. 2025, https://doi.org/10.17775/CSEEJPES.2022.07110.

[4] Y. Gu and T. C. Green, "Power System Stability With a High Penetration of Inverter-Based Resources," *Proceedings of the IEEE*, vol. 111, no. 7, pp. 832–853, July 2023, https://doi.org/10.1109/JPROC.2022.3179826.

[5] J. Wu, M. Han, and M. Zhan, "Transient synchronization stability of photovoltaics integration by singular perturbation analysis," *Frontiers in Energy Research*, vol. 12, Feb. 2024, Art. no. 1332272, https://doi.org/10.3389/fenrg.2024.1332272.

[6] Y. Zhang, F. Liu, and Q. Guo, "Critical clearing time sensitivity of power systems with high power electronic penetration," *iEnergy*, vol. 4, no. 1, pp. 3–15, Mar. 2025, https://doi.org/10.23919/IEN.2025.0001.

[7] X. Wang *et al.*, "Fast Critical Clearing Time Calculation for Power Systems with Synchronous and Asynchronous Generation." arXiv, Mar. 15, 2025, https://doi.org/10.48550/arXiv.2503.12132.

[8] R. Mishan, X. Fu, C. Hingu, and M. Ben-Idris, "Impacts of Inertia and Photovoltaic Integration on Existing and Proposed Power System Transient Stability Parameters," *Energies*, vol. 18, no. 11, June 2025, Art. no. 2915, https://doi.org/10.3390/en18112915.

[9] B. H. Alajrash, M. Salem, M. Swadi, T. Senjyu, M. Kamarol, and S. Motahhir, "A comprehensive review of FACTS devices in modern power systems: Addressing power quality, optimal placement, and stability with renewable energy penetration," *Energy Reports*, vol. 11, pp. 5350–5371, June 2024, https://doi.org/10.1016/j.egyr.2024.05.011.

[10] R. Mihalic, M. Eremia, and B. Blazic, "Static Synchronous Compensator – Statcom," in *Advanced Solutions in Power Systems: HVDC, FACTS, and Artificial Intelligence*, John Wiley & Sons, Ltd, 2016, pp. 459–525.

[11] M. O. abed el-Raouf, S. A. A. Mageed, M. M. Salama, M. I. Mosaad, and H. A. AbdelHadi, "Performance Enhancement of Grid-Connected Renewable Energy Systems Using UPFC," *Energies*, vol. 16, no. 11, May 2023, Art. no. 4362, https://doi.org/10.3390/en16114362.

[12] P. K. Iyambo and R. Tzoneva, "Transient stability analysis of the IEEE 14-bus electric power system," in *AFRICON 2007*, Sept. 2007, pp. 1–9, https://doi.org/10.1109/AFRCON.2007.4401510.

[13] B. Bouhadouza, T. Bouktir, and A. Bourenane, "Transient Stability Augmentation of the Algerian South-Eastern Power System including PV Systems and STATCOM," *Engineering, Technology & Applied Science Research*, vol. 10, no. 3, pp. 5660–5667, June 2020, https://doi.org/10.48084/etasr.3433.

[14] N. E. Akpeke, C. M. Muriithi, and C. Mwaniki, "Contribution of FACTS Devices to the Transient Stability Improvement of a Power System Integrated with a PMSG-based Wind Turbine," *Engineering, Technology & Applied Science Research*, vol. 9, no. 6, pp. 4893–4900, Dec. 2019, https://doi.org/10.48084/etasr.3090.

[15] M. Asad, M. Faizan, P. Zanchetta, and J. Á. Sánchez-Fernández, "FACTS Controllers' Contribution for Load Frequency Control, Voltage Stability and Congestion Management in Deregulated Power Systems over Time: A Comprehensive Review," *Applied Sciences*, vol. 15, no. 14, July 2025, Art. no. 8039, https://doi.org/10.3390/app15148039.

[16] M. Amroune and T. Bouktir, "Effects of Different Parameters on Power System Transient Stability Studies," *Journal of Applied Science and Advanced Engineering*, vol. 1, no. 1, pp. 28–33, 2014.

[17] F. Milano, "An open source power system analysis toolbox," *IEEE Transactions on Power Systems*, vol. 20, no. 3, pp. 1199–1206, Aug. 2005, https://doi.org/10.1109/TPWRS.2005.851911.

[18] M. Drif, M. Bahri, and D. Saigaa, "A novel equivalent circuit-based model for photovoltaic sources," *Optik*, vol. 242, Sept. 2021, Art. no. 167046, https://doi.org/10.1016/j.ijleo.2021.167046.

[19] F. Milano, *Power System Modelling and Scripting*. Berlin, Heidelberg: Springer, 2010.

[20] Y. Sun, J. Ma, J. Kurths, and M. Zhan, "Equal-area criterion in power systems revisited," *Proceedings of the Royal Society A: Mathematical, Physical and Engineering Sciences*, vol. 474, no. 2210, Feb. 2018, Art. no. 20170733, https://doi.org/10.1098/rspa.2017.0733.

[21] M. Chouki, H. Belila, and H. Zaimen, "Study of Flexible AC Transmission Systems and Static Var Compensator and Their Behavior on Power and Voltage Control in Transmission Networks," *Mathematical Modelling of Engineering Problems*, vol. 12, no. 7, pp. 2513–2521, July 2025, https://doi.org/10.18280/mmep.120729.